Oriented nucleosome binding by the pioneer factor ELF2

Tianyi Xiao[1], Caillan Crowe-McAuliffe[2], Moritz Ochmann[2], Fangjie Zhu[3], Maria Osmala[4], Connor Rogerson[1], Patrick Cramer[2], Christian Dienemann[2], Jussi Taipale[1,4,5]

[1]Department of Biochemistry, University of Cambridge, United Kingdom
[2]Max-Planck Institute for Multidisciplinary Sciences, Department of Molecular Biology, Göttingen, Germany
[3]Haixia Institute of Science and Technology, Fujian Agriculture and Forestry University, Fuzhou, Fujian, China
[4]Applied Tumor Genomics Program, Faculty of Medicine, University of Helsinki, Finland
[5]Department of Medical Biochemistry and Biophysics, Karolinska Institutet, Sweden

Abstract

Pioneer factors are transcription factors that are important for stem cell pluripotency, cell reprogramming and differentiation, due to their ability to bind to nucleosomes at closed chromatin regions. ELF2 is an ETS family pioneer factor that has a strong preference for oriented binding on nucleosomes (Zhu et al., 2018). On nucleosomes, ELF2 preferentially binds to a composite head-to-tail dimeric motif with a 2 bp spacing between the GGAA core sequences. In this study, we investigated the interaction between ELF2 and a nucleosome using single-particle cryo-electron microscopy (cryo-EM) analysis. The ELF2-nucleosome structure shows two ELF2 proteins bound to the nucleosome cooperatively at superhelical location +4. The recognition α4 helices of both ELF2 monomers dock into the major groove of DNA at the core GGAA motifs, and unwrap the nucleosome by approximately four helical turns. The unwrapping almost completely exposes one histone H2A:H2B dimer, which dissociates in a subset of particles to form an ELF2-bound hexasome. Genome-wide mapping of the ELF2 composite motifs shows that they are highly enriched downstream of transcription start sites (TSS), oriented in such a way that the TSS becomes accessible upon ELF2 binding to a nucleosome. ELF2 binding is also expected to increase the inter-nucleosome distance, and recruit chromatin remodelers that can recognize exposed histone surfaces or the hexasome. Our results suggest that ELF2 can open chromatin in an oriented fashion, facilitating chromatin remodeling and transcription initiation.

Introduction

A nucleosome is the basic unit of DNA packaging, it consists of ~ 147 bp of DNA, and an octamer of two copies of each of histones H2A, H2B, H3 and H4. For a canonical nucleosome, DNA wraps 1 ¾ turns around the octamer in a left-handed manner (Luger et al., 1997). The formation of a nucleosome distorts the canonical B-form of DNA by bending the DNA towards the histone octamer. Assembly of nucleosomes on free DNA to form chromatin prevents transcriptional initiation (Kornberg and Lorch, 2020), and generally decreases the accessibility of DNA for protein binding (Mansisidor and Risca, 2022).

Transcription factors (TFs) are proteins that can recognise and bind to specific DNA sequences and regulate transcription (Lambert et al., 2018). Whereas all TFs can bind free DNA, only a subset of TFs, the pioneer factors, can bind to nucleosomal DNA and activate transcription in closed chromatin regions (Cirillo et al., 2002; Iwafuchi-Doi, 2019; Zaret and Mango, 2016; Zhu et al., 2018). Pioneer factors are important in multiple cellular functions including development, differentiation and cellular reprogramming, and some pioneer factors have also been linked to pathological conditions such as cancer (Caravaca et al., 2013; Iwafuchi-Doi and Zaret, 2016; Riggi et al., 2010; Soufi et al., 2015; Sunkel and Stanton, 2021).

A very large number of studies have investigated the structural basis of the interaction between TFs and DNA using X-ray crystallography. However, despite the importance of the nucleosome and pioneer factors in biology and medicine, much fewer structural studies have focused on the interactions between TFs and nucleosomes. Biochemical studies have established that there are five major modes of TF-nucleosome interaction, a gyre spanning, periodic binding, dyad binding (Zhu et al., 2018) and end binding modes (Li et al., 2005; Polach and Widom, 1995; Zhu et al., 2018), as well as an oriented binding mode, where the TF binding motif shows orientational preference relative to the nucleosome (Sherwood et al., 2014; Zhu et al., 2018). Recently, several investigators, including us, have used cryo-EM to study pioneer factor-nucleosome interactions (Dodonova et al., 2020; Guan et al., 2023; Lian et al., 2024; Michael et al., 2023, 2020; Nishimura et al., 2022; Sinha et al., 2023), identifying the molecular basis of the end-binding and periodic binding modes. However, the molecular basis of the oriented binding of TFs to nucleosomes has not been investigated previously. In this work, we have studied the mechanism by which the ETS family TF, ELF2, binds to nucleosomes in an oriented manner.

Results

To investigate the binding of ELF2 to nucleosomal DNA, first investigated the optimal binding position of ELF2 on nucleosomes. Read-level and motif-mapping analysis of earlier nucleosome consecutive affinity purification SELEX (NCAP-SELEX) data from Zhu et al., 2018 using MOODS (Korhonen et al., 2009) revealed that ELF2 strongly preferred binding close to superhelical location +4 (SHL +4) position on the forward strand of nucleosomal DNA (**Fig. 1a**). Other ETS proteins tested, including class I (ERG, FLI1, FEV), class II (ELF1, ELF4, ELF5) and class III (SPIB) ETS proteins also preferred to bind to this position (**Fig. S1**). Our analysis also established that on nucleosomes, ELF2 prefers to bind to a double motif "CCGGAAGCGGAAGT" (see (Jolma et al., 2013)), where the two GGAA core sequences are located in a head-to-tail orientation with a 2 bp gap (ELF2-HT2 motif hereafter). We then used Cryo-EM to determine the structure of a complex of two human ELF2 DNA-binding domains (DBDs) bound to a nucleosome containing the double ELF2-HT2 motif. The ELF2-HT2 motif was placed in the preferred position within a Widom 601 nucleosome positioning sequence (**Fig. 1b, c**; (Lowary and Widom, 1998)).

ELF2-nucleosome structure

Nucleosomes were reconstituted *in vitro* by gradual lowering of the salt concentration (dialysis), using histone octamer from *Xenopus laevis* and the designed DNA sequence. A 20-fold excess of purified ELF2 DBD was then added to the reconstituted nucleosomes, and the complex incubated for 25 minutes at room temperature (see **Methods** for details). The sample was then plunge-frozen in ethane and cryo-EM data were acquired from the frozen grids.

After initial cleanup steps to remove poorly-aligning particles, 1,179,230 particles were obtained and classified as described in **Methods**. Serial classification for nucleosomes yielded a 3D class consisting of 103,825 particles that was refined to a 3.8 Ångstrom (Å) map of a nucleosome with extra density at SHL +4. The extra density corresponded to two ELF2 proteins and a straight DNA strand exiting the nucleosome (**Fig. 2a**). A weaker density was observed at SHL +4 to +7, probably originating from a strand of free DNA that binds the exposed H2A:H2B dimer in trans (**Fig. S2a**). Of the main class, only ~ 4% of particles represented a free nucleosome without bound ELF2 (**Fig. S2b**), indicating that under the

conditions tested, ELF2 has a high occupancy, and its binding to nucleosomes is relatively stable.

Due to the flexibility of DNA, approximately two helical turns of DNA were not visible at the unwrapped end of the DNA (SHLs +6 and +7 in **Fig. 2a**). The flexibility of the DNA tail was represented by several 3D classes, where the DNA exits the nucleosome at slightly different angles both tangentially (up-down in **Fig. S3a**) and in direction perpendicular to the plane of the nucleosome disc (left-right in **Fig. S3b**). Due to this flexibility, the resolution of the ELF2-bound regions was improved by refining the density locally, resulting in a 5.4 Å reconstruction of this region (see **Methods**).

To build the model shown in **Fig. 2b**, we fitted the structure of a nucleosome (PDB 6FQ5) and an Alphafold 2.0-predicted structure of ELF2 DBD into the cryo-EM density of map shown in **Fig. 2a**. The structure shows two ELF2 DBDs bound to DNA at SHL +4 opposite to the dyad (**Fig. 2d**). The recognition helices of both ELF2 DBDs were bound to the major groove of DNA at the expected GGAA sites, with the two proteins bound to DNA on opposite sides of the DNA helix. On a fully wound nucleosome, the first ELF2 binding site (the one that is closer to the nucleosome in the structure) is largely accessible from the solvent side, whereas the second site is occluded in such a way that an ELF2 bound to it would clash with the other DNA gyre (**Fig. S4**), suggesting a consecutive binding mechanism for the two ELF2 proteins.

Unwrapping, local interactions

In the structure (**Fig. 3a**), nucleosomal DNA unwraps from the first bound ELF2 at SHL +4 to the end, four helical turns away (at SHL +7), with two of the helical turns (at SHL +4 and +5) being resolved in the structure. Approximately 40 bp of DNA is fully detached from the nucleosome. This suggests that binding of ELF2 to the nucleosome induces unwrapping to the nucleosomal DNA from SHL +4 to +7. To rule out artefacts due to sample preparation, and to test whether ELF2 binding indeed increases DNA accessibility at sites distal to the bound motifs, we introduced an EcoRV cleavage site to the unwrapped end of DNA. EcoRV was chosen based on its reported structure (Perona and Martin, 1997); it interacts with DNA extensively, binding to both sides of DNA, requiring > 300° degree of access around the cylinder of DNA. EcoRV is thus unable to recognize its cleavage site if the DNA segment is stably wound around a nucleosome.

Consistently, we found that when DNA is wrapped around the nucleosome, DNA is efficiently protected from EcoRV digestion, whereas pre-incubation with ELF2 enables cleavage of a DNA containing an EcoRV site distal to the ELF2 dual motif (**Fig. 3b**).

Potential mechanism for oriented nucleosome recognition

The structure we obtained also suggests a mechanism for the orientational preference of ELF2 nucleosome binding. The ELF2 monomer bound to the second site is oriented in such a way that a lysine, K229, is located near the phosphate backbone of the other gyre of DNA at SHL -4 (**Fig. 3c**). The side-chain of this lysine is not resolved in the structure, but it could reach within 4.5 Å of the phosphate at base 35, indicating a potential electrostatic interaction.

ELF2 binding can release an H2A:H2B dimer

Unwrapping of DNA due to binding of the two ELF2 proteins also exposes one of the H2A:H2B dimers to solvent (**Fig. 3d**). Almost all contacts between this H2A:H2B dimer and DNA are lost compared to those observed in the canonical nucleosome structure (**Table I**; **Fig. 3e**). Upon ELF2 binding, the predicted binding surface and solvation free energy between H2A:H2B and DNA decreased by 85% and 76%, respectively, indicating much weaker binding of the H2A:H2B dimer onto DNA after the partial unwrapping of DNA. Consistently, we observed a class of 23,778 particles that was similar to the major class except that it contained a hexasome instead of a full histone octamer (**Fig. 3f**). In this class, the ELF2-bound DNA was unwrapped from SHL +4 to the end, and the H2A:H2B dimer bound to the released DNA segment was dissociated from the complex (**Fig. 3f**).

Potential role for ELF2 in releasing the TSS from the +1 nucleosome

To understand the biological role of the ELF2 nucleosome binding, we mapped the ELF2-HT2 motif to the human genome, and studied its location relative to the TSS. We found that the motif was enriched at around 6 bp downstream from TSS in one orientation. Binding of ETS TFs to this motif and unwrapping of nucleosomal DNA would result in the TSS position being released from a nucleosome (**Fig. 4a**, shaded region). Comparison with YY1, a TF whose motif is known to be oriented at 20-30 bp downstream of TSS (Dudnyk et al., 2024; Sahu et al., 2022) indicated that the extent of oriented enrichment was similar

between ELF-HT2 and the most strongly oriented TF motif that has been previously described (YY1). As control, single ETS motifs show weaker orientational preference relative to the TSS (see also (Sahu et al., 2022), **Fig. 4a**), suggesting that the double motif (ETS-HT2) may release the DNA segment containing the TSS (**Fig. 4a**, shaded region), and thus have a specific and novel role in transcriptional regulation.

Discussion

In this work, we have solved the structure of ELF2 bound to the nucleosome. We found that by binding in a head-to-tail dimeric fashion, ELF2 protein unwraps the nucleosome by four superhelical turns, exposing 40 bp of free DNA and the H2A:H2B interface. Structures of many pioneer factor-nucleosome interactions have been described in recent publications (see, for example (Dodonova et al., 2020; Guan et al., 2023; Lian et al., 2024; Michael et al., 2023, 2020; Nishimura et al., 2022; Sinha et al., 2023)). Most pioneer factors described bind near to the end of nucleosomal DNA. However, in this study, we examined ELF2, which prefers to bind at around SHL +4, opposite of the dyad. Compared to some other pioneer factors such as CLOCK (Michael et al., 2023), ELF2 binds to DNA further into the nucleosome, and unwraps more DNA. The ELF2 dimer motif that is preferentially bound on a nucleosome is enriched downstream of the TSS in such a way that binding to the site would expose the TSS, suggesting that the unwrapping mechanism we discovered may promote the initiation of transcription.

Biological role of ETS factors

The ETS family is a large TF family found only in animals. Several ETS family members have central roles in development and disease. For example, the class I ETS factors ERG, ETV1 and ETV4 are linked to prostate cancer (Delattre et al., 1992; Hsu et al., 2004). The ELF family, in turn, has been reported to have important roles in immune and blood cell development and function (Choi et al., 2011). We show here that the nucleosome-bound ELF2-HT2 motif is bound by many members of this family (**Fig. S1**), suggesting that ELF2, and ETS factors more broadly would function as pioneer factors, destabilizing nucleosomes and increasing DNA accessibility and transcription.

Nucleosome unwrapping & chromatin modifications

The mechanism of nucleosome unwrapping observed in this study is based on binding energy, as it involves no enzymes or ATP hydrolysis. As the two ELF2 proteins bind to opposite sides of DNA, they cannot simultaneously bind to nucleosomal DNA. We propose that one ELF2 binds to the first binding site, pulling DNA away from the histones without completely releasing the DNA. This allows the second ELF2 to bind to the second site, leading to unwrapping of the DNA end. After ELF2 binding and nucleosome

unwrapping, DNA stays in an unwrapped state because the second ELF2 prevents re-wrapping of the nucleosome. This mechanism would explain how ELF2 can access an optimal motif present at an optimal position. However, in the genome, nucleosome positions vary, and the first binding site will often be occluded. Even in that case, the binding of the ELF2 proteins to opposite sides of DNA would still ensure that one of the sites would be accessible for binding. We propose that such motifs, which enable binding to both sides of DNA, will be a general mechanism that will allow pioneer factors to access nucleosomal DNA irrespective of the rotational positions of their recognition sequence(s). In addition to direct binding to wrapped DNA, ELF2 can also bind to nucleosomes affected by spontaneous local conformational fluctuations (DNA breathing) that temporarily expose nucleosomal DNA ends (Culkin et al., 2017; Möbius et al., 2006; Polach and Widom, 1995).

Oriented binding

Wrapping of DNA to nucleosomes breaks the rotational (pseudo)symmetry of the DNA molecule, allowing some TFs, such as ELF2, to prefer to bind to nucleosomes in an oriented fashion. Prior to the present work, the mechanism of oriented binding was not understood, as it has not been studied in structural detail. We find here that ELF2 has a lysine residue that can reach out to the phosphate backbone of the opposite DNA gyre. It is therefore speculated that interacting with the phosphates stabilizes ELF2 binding on the second binding site, promoting ELF2 dimer binding in this preferred orientation. If the motif is found in reverse complement (TTCC instead of GGAA), the ELF2 protein would rotate 180 degrees, orienting the lysine away from the other DNA gyre. Oriented binding allows TFs to position nucleosomes precisely relative to their binding motif. We propose that this mechanism is important in positioning of nucleosomes relative to the TSS, and possibly also in setting the boundaries of open chromatin regions in general.

Hexasome and chromatin remodeling

We found here that after ELF2 binding unwraps a nucleosome, the octamer becomes unstable and in some cases dissociates partially, with one H2A:H2B dimer dissociating, which yields a hexasome. Hexasomes comprise around 110 bp DNA wrapped around six histones (Arimura et al., 2012). It has been shown previously that hexasomes recruit chromatin remodelers such as INO80 (Hsieh et al., 2022; Zhang et al., 2023). Our finding that

ELF2 binding can lead to hexasome formation thus suggests a potential novel mechanism by which TFs can recruit chromatin remodelers and increase transcription rates.

Role of oriented binding in transcriptional regulation

TFs recognise specific motifs on DNA and regulate transcription via transcriptional activation domains (Alerasool et al., 2022). Most TFs do not require strict positioning in promoters or enhancers (Sahu et al., 2022). For example, single ETS motifs with core sequence GGAA are broadly located upstream of the TATA box, between TATA box and TSS, and downstream of TSS. By contrast, we find here that the ETS-HT2 dimer motifs are preferentially oriented, and located downstream of the TSS positioned in such a way that the TSS DNA sequence would be released from a nucleosome (**Fig. 4a**).

Unwrapping of nucleosomes by ELF2-DNA interaction generates free DNA for other non-pioneer TF to bind to, and exposes histone H2A:H2B surfaces that are normally buried by nucleosomal DNA. Based on these findings, we propose a model where the ELF2 or other ETS factor binding at the ETS-HT2 sites positioned downstream of a TSS increases transcription by a novel mechanism consisting of three separate actions: 1) increasing DNA accessibility at the TSS, 2) positioning the +1 nucleosome, and 3) modifying the +1 nucleosome by formation of a hexasome (**Fig. 4b**). The proposed novel mechanism differs from the classical activator model in two ways: it critically depends on precise positioning and orientation of the motif, and enables TFs without transcriptional activator domains to activate transcription.

In summary, we describe here the structure of an ETS factor ELF2 bound to nucleosomes as a dimer. Our work is the first structural study of a TF accessing nucleosomes in an oriented fashion, binding in a mode that enables precise control of nucleosome positioning and local DNA accessibility.

Methods

DNA ligand design

The nucleosomal DNA sequence used for the structural study included a dual ELF2 binding motif (CCGGAAGCGGAAGT) inserted into the preferred binding position within a Widom 601 core sequence (147 bp). The full sequence of the DNA (DNA1) used in the structural studies (ETS-HT2 motif underlined) was:

5′-
CTGGAGAATCCCGGTCTGCAGGCCGCTCAATTGGTCGTAGACAGCTCTAGCACCGCTTAAAC
GCACGTACGCGCTGTCCCCCGCGTTTTAACCGCCAAGGGGATTACTCCGGAAGCGGAAGTTG
TATGTCAGATATATACATCCTGT-3′

The following three DNA sequences, each containing a single EcoRV site were also constructed for the restriction digestion analyses. The sequence (DNA2) with ELF2-HT2 motif (underlined) and EcoRV site (**bold**) was:

5′-
CTGGAGAATCCCGGTCTGCAGGCCGCTCAATTGGTCGTAGACAGCTCTAGCACCGCTTAAAC
GCACGTACGCGCTGTCCCCCGCGTTTTAACCGCCAAGGGGATTACTCCGGAAGCGGAAGTTG
TATGTCA**GATATC**TACATCCTGT-3′

The sequence (DNA3) with only the first ELF2 motif (underlined) and EcoRV site (**bold**) was:

5′-
CTGGAGAATCCCGGTCTGCAGGCCGCTCAATTGGTCGTAGACAGCTCTAGCACCGCTTAAAC
GCACGTACGCGCTGTCCCCCGCGTTTTAACCGCCAAGGGGATTACTCCGGAAGCGTTAGTTG
TATGTCA**GATATC**TACATCCTGT-3′

and the sequence (DNA4) with only the second ELF2 motif (underlined) and EcoRV site (**bold**) was:

5′-
CTGGAGAATCCCGGTCTGCAGGCCGCTCAATTGGTCGTAGACAGCTCTAGCACCGCTTAAAC
GCACGTACGCGCTGTCCCCCGCGTTTTAACCGCCAAGGGGATTACTCCATAAGCGGAAGTTG
TATGTCA**GATATC**TACATCCTGT-3′

The fragments were constructed from one single-stranded full-length oligonucleotide using PCR (Phusion polymerase, 35 cycles, annealing 57°C 10s, elongation 72°C 36s, denaturation 98°C 15s) with the following Forward primer (common) CTGGAGAATCCCGGTCTGC. The reverse primer Rev1 ACAGGATGTATATATCTG was used for DNA1, and Rev2 ACAGGATGTAGATATCTG for DNAs 2-4. All DNAs 1-4 were purified by

anion exchange using ResourceQ 1 ml column (Cytiva), followed by isopropanol precipitation.

ELF2 protein expression & purification

DNA-binding domain fragment of human ELF2 (encoding amino-acids 182-326; sequence: TQQSPISNGSPELGIKKKPREGKGNTTYLWEFLLDLLQDKNTCPRYIKWTQREKGIFKLVDSKAVSKLWGK HKNKPDMNYETMGRALRYYYQRGILAKVEGQRLVYQFKDMPKNIVVIDDDKSETCNEDLAGTTDEKSLE RVSLS) were cloned by Genscript and purified by Protein Science Facility at Karolinska Institutet.

Histone octamer expression and purification

Xenopus laevis histones H2A, H2B, H3, and H4 were expressed and purified as described previously (Dyer et al., 2003; Farnung et al., 2017). In brief, each histone was expressed in BL21 (RIL) DE3 (Agilent) for 3 h at 37°C induced by 1 mM IPTG. Histones were extracted and purified from inclusion bodies. Cell pellets were resuspended (in 50 mM Tris-HCl pH 7.5 (@ 20°C), 100 mM NaCl, 1 mM EDTA, 2 mM DTT, 0.284 µg ml^{-1} leupeptin, 1.37 µg ml^{-1} pepstatin A, 0.17 mg ml^{-1} PMSF, and 0.33 mg ml^{-1} benzamidine), lysed by sonication and pelleted by centrifugation. The pellet was washed repeatedly (with and without 1% (v/v) Triton X-100), before the histones were extracted from the inclusion bodies using DMSO followed by unfolding buffer (7 M guanidine hydrochloride, 20 mM Tris-HCl pH 7.5 (at 20°C), 10 mM DTT). The resuspended histones were buffer exchanged (using HiPrep 26/10 Desalting column (Cytivia) to 7 M deionized urea, 20 mM sodium acetate pH 5.2, 200 mM NaCl, 1 mM EDTA, 2 mM DTT) and purified with a HiTrap Q HP column (Cytivia) followed by a HiPrep SP FF 16/10 column (Cytivia). Fractions containing purified histones were dialyzed against 15 mM Tris-HCl pH 7.5 (at 20°C) and 2 mM DTT before being aliquoted, snap-frozen, and lyophilized before storage at -70°C. Histone octamer were formed as described (Dyer et al., 2003). Histones H2A, H2B, H3, and H4 were resuspended in unfolding buffer (7 M guanidine hydrochloride, 20 mM Tris-HCl pH 7.5 (at 20°C), 10 mM DTT), mixed at a molar ratio of 1.2:1.2:1:1, respectively, and dialysed three times against refolding buffer (2 M NaCl, 20 mM Tris-HCl pH 7.5 (at 4°C), 1 mM EDTA, 5 mM β-mercaptoethanol) at 4°C. The formed octamer was purified with a HiLoad 16/600 Superdex 200 pg column (Cytiva). Fractions

containing the histones in a equimolar ratio, analysed by SDS-PAGE and Coomassie staining, were pooled, concentrated with a 10,000 MWCO Amicon Ultra Centrifugal Filter (Merck), quantified by 280 nm absorption, and stored at 4°C for use.

Nucleosome reconstitution

Nucleosome was reconstituted from histone octamer and DNA template at 1.1:1 molar ratio by dialysis from a high salt buffer ("RB high"; (Dyer et al., 2003); 1 mM EDTA, 2 M NaCl, 2 mM DTT in 20 mM HEPES, pH 7.5) to a low salt buffer ("RB low"; 1 mM EDTA, 30 mM NaCl, 2 mM DTT in 20 mM HEPES, pH 7.5) over 24 hours (Dodonova et al., 2020; Dyer et al., 2003). Successful reconstitution of the nucleosome was validated by electrophoresis in an 3% agarose gel.

Cryo-EM sample preparation & data acquisition

Nucleosome-ELF2 samples were prepared by incubating the reconstituted nucleosomes (at 200 nM concentration) with ELF2 protein (1:20 molar ratio) at 25°C for 25 min. Subsequently, 3.2 µl samples of the solution were applied onto EM grids (Quantifoil, R 1.2/1.3 Cu 300 mesh) that had been glow discharged with PELCO easiGlow for 60 seconds in Vitrobot Mark IV chamber at 4°C and 90% humidity. The grid was then blotted for 3 seconds with -5 blotting force and vitrified by plunging into liquid ethane.

Single particle data was collected on Titan Krios G2 microscope (FEI) equipped with a K3 Summit direct electron detector (Gatan). Data was collected using EPU software (ThermoFisher), at nominal magnification of 130,000 x, with a pixel size of 0.652 Å, defocus range from -2.4 to -0.8 at 0.2 intervals, energy filter of 20 eV, and total electron dose of 51.09 electrons/Å^2 distributed across 44 movie frames.

Data processing and analysis

Contrast-transfer functions for micrographs were estimated using Warp (Tegunov and Cramer, 2019), and particles were picked using the RELION 4.0 template picking tool using 2D references generated from a nucleosome map (Kimanius et al., 2021; Scheres, 2012). To speed up the initial particle cleanup, the picked particles were extracted and binned to a pixel size of 2.608 Å, and cleaned up using cryoSPARC (Punjani et al., 2017) with several rounds of 2D classification, ab-initio reconstruction and heterogeneous refinement.

The cleaned up particles were then imported back into RELION and further cleaned up to include only classes containing a nucleosome by 3D classifications and 3D refinements. A local mask was then made on the trans-DNA at SHL +4 to +7 and particles were substracted to the local mask region, and a 3D classification performed locally with the subtracted particles. The classes with trans-DNA and the class without trans-DNA were selected, and particles re-extracted with pixel size of 1.304 Å.

Local ELF region was classified with subtracted particles and classes with two ELF2 bound to DNA were selected. The selected particles were subsequently refined locally, followed by another round of 3D classifications. For an overview of data processing workflow, see **Fig. S5**, for Fourier Shell Correlation (FSC) curves of refined maps, see **Fig. S6**.

Model fitting and validation

A nucleosome model (6fq5, (Bilokapic et al., 2018)) was fitted into the ELF2-nucleosome cryo-EM map in ChimeraX (Meng et al., 2023). The Alphafold prediction (Varadi et al., 2022) of ELF2 DBD was used for initial rigid body fitting. To account for the unwrapped DNA, an ideal B-form DNA double helix was created in the program Coot (Emsley et al., 2010) using the designed DNA sequence and fitted into density. The modified nucleosome structure with the two ELF2 proteins was refined using the program ISOLDE (Croll, 2018) and validated using Phenix (Afonine et al., 2018). Solvation free energy and interface area between histones and DNA was calculated using PISA (Krissinel and Henrick, 2007).

Electrophoretic mobility shift assay

All steps of EMSA were performed on ice, with running buffer pre-chilled to 4°C. EMSA was performed on an 8% Tris-Glycine gel (Thermo Fisher). 1X Tris-Glycine Native Running Buffer (Thermo Fisher) was used as a running buffer. The gel was pre-rinsed with Running Buffer before assembly of the gel tank. Tris-Glycine Native Sample Buffer (Thermo Fisher) was added to ELF2-nucleosome reaction and mixed by pipetting. Samples were then loaded onto gel and ran on ice at 125V for 2 h. The gel was then stained in SYBR-gold (Thermo Fisher) and visualized using Bio-Rad Imager (**Fig. S7**).

Restriction enzyme digestion assay

Nucleosomes were reconstituted with modified DNA ligand containing an EcoRV site. Reconstituted nucleosome (containing 0.5 µg of DNA) was then incubated with ELF2 at 1:20 molar ratio at 25 °C for 10 minutes, followed by addition of 1.5 U of EcoRV (NEB), and further incubation of the mixture for 15 min at 37 °C. To stop the reaction, Proteinase K and SDS were added to 0.2 mg/ml and 0.5% final concentrations, respectively, followed by incubation at 55 °C for 10min. The DNA fragments were then analyzed by electrophoresis at a 3% agarose gel (**Fig. S8**).

Genome mapping of motifs

TF motifs (ETS dual motif, ELF2 single motif , YY1 motif) were obtained from (Jolma et al., 2013; Yin et al., 2017; Zhu et al., 2018), and their positioning on human genome (hg38) was determined using MOODS (Korhonen et al., 2009). The relative positions of motifs relative to TSS was determined using HOMER (Heinz et al., 2010). Positioning of motifs against TSS was plotted with python Plotly with a 10 bp sliding window.

ACKNOWLEDGMENTS

We thank Kenneth Jones for technical assistance, and Dr. Ekaterina Morgunova and Yinan Chen for critical review of the manuscript. Part of this work was facilitated by the Protein Science Facility at Karolinska Institutet/SciLifeLab (http://ki.se/psf) and we would like to thank Dr. Henry Ampah-Korsah and Dr. Emilia Strandback for the assistance. We thank Mr Lee R. Cooper, Dr Steve W. Hardwick and Dr Dimitri Y. Chirgadze for their assistance using the Cryo-EM Facility at the Department of Biochemistry, University of Cambridge. This work was supported by the Max Planck Society, Cancer Research UK (Grant number RG99643) and UK Research and Innovation (Biotechnology and Biological Sciences Research Council G107673 and Medical Research Council G105296).

REFERENCES

Afonine, P.V., Poon, B.K., Read, R.J., Sobolev, O.V., Terwilliger, T.C., Urzhumtsev, A., Adams, P.D., 2018. Real-space refinement in PHENIX for cryo-EM and crystallography. Acta Cryst D 74, 531–544. https://doi.org/10.1107/S2059798318006551

Alerasool, N., Leng, H., Lin, Z.-Y., Gingras, A.-C., Taipale, M., 2022. Identification and functional characterization of transcriptional activators in human cells. Molecular Cell 82, 677-695.e7. https://doi.org/10.1016/j.molcel.2021.12.008

Arimura, Y., Tachiwana, H., Oda, T., Sato, M., Kurumizaka, H., 2012. Structural Analysis of the Hexasome, Lacking One Histone H2A/H2B Dimer from the Conventional Nucleosome. Biochemistry 51, 3302–3309. https://doi.org/10.1021/bi300129b

Bilokapic, S., Strauss, M., Halic, M., 2018. Structural rearrangements of the histone octamer translocate DNA. Nat Commun 9, 1330. https://doi.org/10.1038/s41467-018-03677-z

Caravaca, J.M., Donahue, G., Becker, J.S., He, X., Vinson, C., Zaret, K.S., 2013. Bookmarking by specific and nonspecific binding of FoxA1 pioneer factor to mitotic chromosomes. Genes Dev 27, 251–260. https://doi.org/10.1101/gad.206458.112

Choi, H.-J., Geng, Y., Cho, H., Li, S., Giri, P.K., Felio, K., Wang, C.-R., 2011. Differential requirements for the Ets transcription factor Elf-1 in the development of NKT cells and NK cells. Blood 117, 1880–1887. https://doi.org/10.1182/blood-2010-09-309468

Cirillo, L.A., Lin, F.R., Cuesta, I., Friedman, D., Jarnik, M., Zaret, K.S., 2002. Opening of Compacted Chromatin by Early Developmental Transcription Factors HNF3 (FoxA) and GATA-4. Molecular Cell 9, 279–289. https://doi.org/10.1016/S1097-2765(02)00459-8

Croll, T.I., 2018. ISOLDE: a physically realistic environment for model building into low-resolution electron-density maps. Acta Cryst D 74, 519–530. https://doi.org/10.1107/S2059798318002425

Culkin, J., de Bruin, L., Tompitak, M., Phillips, R., Schiessel, H., 2017. The role of DNA sequence in nucleosome breathing. Eur. Phys. J. E 40, 106. https://doi.org/10.1140/epje/i2017-11596-2

Delattre, O., Zucman, J., Plougastel, B., Desmaze, C., Melot, T., Peter, M., Kovar, H., Joubert, I., de Jong, P., Rouleau, G., Aurias, A., Thomas, G., 1992. Gene fusion with an ETS DNA-binding domain caused by chromosome translocation in human tumours. Nature 359, 162–165. https://doi.org/10.1038/359162a0

Dodonova, S.O., Zhu, F., Dienemann, C., Taipale, J., Cramer, P., 2020. Nucleosome-bound SOX2 and SOX11 structures elucidate pioneer factor function. Nature 580, 669–672. https://doi.org/10.1038/s41586-020-2195-y

Dudnyk, K., Cai, D., Shi, C., Xu, J., Zhou, J., 2024. Sequence basis of transcription initiation in the human genome. Science 384, eadj0116. https://doi.org/10.1126/science.adj0116

Dyer, P.N., Edayathumangalam, R.S., White, C.L., Bao, Y., Chakravarthy, S., Muthurajan, U.M., Luger, K., 2003. Reconstitution of Nucleosome Core Particles from Recombinant Histones and DNA, in: Methods in Enzymology, Chromatin and Chromatin Remodeling Enzymes, Part A. Academic Press, pp. 23–44. https://doi.org/10.1016/S0076-6879(03)75002-2

Emsley, P., Lohkamp, B., Scott, W.G., Cowtan, K., 2010. Features and development of Coot. Acta Cryst D 66, 486–501. https://doi.org/10.1107/S0907444910007493

Farnung, L., Vos, S.M., Wigge, C., Cramer, P., 2017. Nucleosome–Chd1 structure and implications for chromatin remodelling. Nature 550, 539–542. https://doi.org/10.1038/nature24046

Guan, R., Lian, T., Zhou, B.-R., Wheeler, D., Bai, Y., 2023. Structural mechanism of *LIN28B* nucleosome targeting by OCT4. Molecular Cell 83, 1970-1982.e6. https://doi.org/10.1016/j.molcel.2023.05.030

Heinz, S., Benner, C., Spann, N., Bertolino, E., Lin, Y.C., Laslo, P., Cheng, J.X., Murre, C.,

Singh, H., Glass, C.K., 2010. Simple combinations of lineage-determining transcription factors prime cis-regulatory elements required for macrophage and B cell identities. Mol Cell 38, 576–589. https://doi.org/10.1016/j.molcel.2010.05.004
Hsieh, L.J., Gourdet, M.A., Moore, C.M., Muñoz, E.N., Gamarra, N., Ramani, V., Narlikar, G.J., 2022. A hexasome is the preferred substrate for the INO80 chromatin remodeling complex, allowing versatility of function. Molecular Cell 82, 2098-2112.e4. https://doi.org/10.1016/j.molcel.2022.04.026
Hsu, T., Trojanowska, M., Watson, D.K., 2004. Ets proteins in biological control and cancer. Journal of Cellular Biochemistry 91, 896–903. https://doi.org/10.1002/jcb.20012
Iwafuchi□Doi, M., 2019. The mechanistic basis for chromatin regulation by pioneer transcription factors. Wiley Interdiscip Rev Syst Biol Med 11, e1427. https://doi.org/10.1002/wsbm.1427
Iwafuchi-Doi, M., Zaret, K.S., 2016. Cell fate control by pioneer transcription factors. Development 143, 1833–1837. https://doi.org/10.1242/dev.133900
Jolma, A., Yan, J., Whitington, T., Toivonen, J., Nitta, K.R., Rastas, P., Morgunova, E., Enge, M., Taipale, M., Wei, G., Palin, K., Vaquerizas, J.M., Vincentelli, R., Luscombe, N.M., Hughes, T.R., Lemaire, P., Ukkonen, E., Kivioja, T., Taipale, J., 2013. DNA-Binding Specificities of Human Transcription Factors. Cell 152, 327–339. https://doi.org/10.1016/j.cell.2012.12.009
Kimanius, D., Dong, L., Sharov, G., Nakane, T., Scheres, S.H.W., 2021. New tools for automated cryo-EM single-particle analysis in RELION-4.0. Biochemical Journal 478, 4169–4185. https://doi.org/10.1042/BCJ20210708
Korhonen, J., Martinmäki, P., Pizzi, C., Rastas, P., Ukkonen, E., 2009. MOODS: fast search for position weight matrix matches in DNA sequences. Bioinformatics 25, 3181–3182. https://doi.org/10.1093/bioinformatics/btp554
Kornberg, R.D., Lorch, Y., 2020. Primary Role of the Nucleosome. Molecular Cell 79, 371–375. https://doi.org/10.1016/j.molcel.2020.07.020
Krissinel, E., Henrick, K., 2007. Inference of Macromolecular Assemblies from Crystalline State. Journal of Molecular Biology 372, 774–797. https://doi.org/10.1016/j.jmb.2007.05.022
Lambert, S.A., Jolma, A., Campitelli, L.F., Das, P.K., Yin, Y., Albu, M., Chen, X., Taipale, J., Hughes, T.R., Weirauch, M.T., 2018. The Human Transcription Factors. Cell 172, 650–665. https://doi.org/10.1016/j.cell.2018.01.029
Li, G., Levitus, M., Bustamante, C., Widom, J., 2005. Rapid spontaneous accessibility of nucleosomal DNA. Nat Struct Mol Biol 12, 46–53. https://doi.org/10.1038/nsmb869
Lian, T., Guan, R., Zhou, B.-R., Bai, Y., 2024. Structural mechanism of synergistic targeting of the CX3CR1 nucleosome by PU.1 and C/EBPα. Nat Struct Mol Biol 1–11. https://doi.org/10.1038/s41594-023-01189-z
Lowary, P.T., Widom, J., 1998. New DNA sequence rules for high affinity binding to histone octamer and sequence-directed nucleosome positioning11Edited by T. Richmond. Journal of Molecular Biology 276, 19–42. https://doi.org/10.1006/jmbi.1997.1494
Luger, K., Mäder, A.W., Richmond, R.K., Sargent, D.F., Richmond, T.J., 1997. Crystal structure of the nucleosome core particle at 2.8 Å resolution. Nature 389, 251–260. https://doi.org/10.1038/38444
Mansisidor, A.R., Risca, V.I., 2022. Chromatin accessibility: methods, mechanisms, and biological insights. Nucleus 13, 238–278. https://doi.org/10.1080/19491034.2022.2143106
Meng, E.C., Goddard, T.D., Pettersen, E.F., Couch, G.S., Pearson, Z.J., Morris, J.H., Ferrin, T.E., 2023. UCSF ChimeraX: Tools for structure building and analysis. Protein Science 32, e4792. https://doi.org/10.1002/pro.4792
Michael, A.K., Grand, R.S., Isbel, L., Cavadini, S., Kozicka, Z., Kempf, G., Bunker, R.D., Schenk, A.D., Graff-Meyer, A., Pathare, G.R., Weiss, J., Matsumoto, S., Burger, L., Schübeler, D., Thomä, N.H., 2020. Mechanisms of OCT4-SOX2 motif readout on nucleosomes. Science 368, 1460–1465. https://doi.org/10.1126/science.abb0074
Michael, A.K., Stoos, L., Crosby, P., Eggers, N., Nie, X.Y., Makasheva, K., Minnich, M.,

Healy, K.L., Weiss, J., Kempf, G., Cavadini, S., Kater, L., Seebacher, J., Vecchia, L., Chakraborty, D., Isbel, L., Grand, R.S., Andersch, F., Fribourgh, J.L., Schübeler, D., Zuber, J., Liu, A.C., Becker, P.B., Fierz, B., Partch, C.L., Menet, J.S., Thomä, N.H., 2023. Cooperation between bHLH transcription factors and histones for DNA access. Nature 619, 385–393. https://doi.org/10.1038/s41586-023-06282-3

Möbius, W., Neher, R.A., Gerland, U., 2006. Kinetic Accessibility of Buried DNA Sites in Nucleosomes. Phys. Rev. Lett. 97, 208102. https://doi.org/10.1103/PhysRevLett.97.208102

Nishimura, M., Takizawa, Y., Nozawa, K., Kurumizaka, H., 2022. Structural basis for p53 binding to its nucleosomal target DNA sequence. PNAS Nexus 1, pgac177. https://doi.org/10.1093/pnasnexus/pgac177

Perona, J.J., Martin, A.M., 1997. Conformational transitions and structural deformability of EcoRV endonuclease revealed by crystallographic analysis11Edited by D. Rees. Journal of Molecular Biology 273, 207–225. https://doi.org/10.1006/jmbi.1997.1315

Polach, K.J., Widom, J., 1995. Mechanism of Protein Access to Specific DNA Sequences in Chromatin: A Dynamic Equilibrium Model for Gene Regulation. Journal of Molecular Biology 254, 130–149. https://doi.org/10.1006/jmbi.1995.0606

Punjani, A., Rubinstein, J.L., Fleet, D.J., Brubaker, M.A., 2017. cryoSPARC: algorithms for rapid unsupervised cryo-EM structure determination. Nat Methods 14, 290–296. https://doi.org/10.1038/nmeth.4169

Riggi, N., Suvà, M.-L., Vito, C.D., Provero, P., Stehle, J.-C., Baumer, K., Cironi, L., Janiszewska, M., Petricevic, T., Suvà, D., Tercier, S., Joseph, J.-M., Guillou, L., Stamenkovic, I., 2010. EWS-FLI-1 modulates miRNA145 and SOX2 expression to initiate mesenchymal stem cell reprogramming toward Ewing sarcoma cancer stem cells. Genes Dev. 24, 916–932. https://doi.org/10.1101/gad.1899710

Sahu, B., Hartonen, T., Pihlajamaa, P., Wei, B., Dave, K., Zhu, F., Kaasinen, E., Lidschreiber, K., Lidschreiber, M., Daub, C.O., Cramer, P., Kivioja, T., Taipale, J., 2022. Sequence determinants of human gene regulatory elements. Nat Genet 54, 283–294. https://doi.org/10.1038/s41588-021-01009-4

Scheres, S.H.W., 2012. RELION: Implementation of a Bayesian approach to cryo-EM structure determination. Journal of Structural Biology 180, 519–530. https://doi.org/10.1016/j.jsb.2012.09.006

Sherwood, R.I., Hashimoto, T., O'Donnell, C.W., Lewis, S., Barkal, A.A., van Hoff, J.P., Karun, V., Jaakkola, T., Gifford, D.K., 2014. Discovery of directional and nondirectional pioneer transcription factors by modeling DNase profile magnitude and shape. Nat Biotechnol 32, 171–178. https://doi.org/10.1038/nbt.2798

Sinha, K.K., Bilokapic, S., Du, Y., Malik, D., Halic, M., 2023. Histone modifications regulate pioneer transcription factor cooperativity. Nature 619, 378–384. https://doi.org/10.1038/s41586-023-06112-6

Soufi, A., Garcia, M.F., Jaroszewicz, A., Osman, N., Pellegrini, M., Zaret, K.S., 2015. Pioneer Transcription Factors Target Partial DNA Motifs on Nucleosomes to Initiate Reprogramming. Cell 161, 555–568. https://doi.org/10.1016/j.cell.2015.03.017

Sunkel, B.D., Stanton, B.Z., 2021. Pioneer factors in development and cancer. iScience 24, 103132. https://doi.org/10.1016/j.isci.2021.103132

Tegunov, D., Cramer, P., 2019. Real-time cryo-electron microscopy data preprocessing with Warp. Nat Methods 16, 1146–1152. https://doi.org/10.1038/s41592-019-0580-y

Varadi, M., Anyango, S., Deshpande, M., Nair, S., Natassia, C., Yordanova, G., Yuan, D., Stroe, O., Wood, G., Laydon, A., Žídek, A., Green, T., Tunyasuvunakool, K., Petersen, S., Jumper, J., Clancy, E., Green, R., Vora, A., Lutfi, M., Figurnov, M., Cowie, A., Hobbs, N., Kohli, P., Kleywegt, G., Birney, E., Hassabis, D., Velankar, S., 2022. AlphaFold Protein Structure Database: massively expanding the structural coverage of protein-sequence space with high-accuracy models. Nucleic Acids Research 50, D439–D444. https://doi.org/10.1093/nar/gkab1061

Yin, Y., Morgunova, E., Jolma, A., Kaasinen, E., Sahu, B., Khund-Sayeed, S., Das, P.K., Kivioja, T., Dave, K., Zhong, F., Nitta, K.R., Taipale, M., Popov, A., Ginno, P.A.,

Domcke, S., Yan, J., Schübeler, D., Vinson, C., Taipale, J., 2017. Impact of cytosine methylation on DNA binding specificities of human transcription factors. Science 356, eaaj2239. https://doi.org/10.1126/science.aaj2239

Zaret, K.S., Mango, S., 2016. Pioneer Transcription Factors, Chromatin Dynamics, and Cell Fate Control. Curr Opin Genet Dev 37, 76–81. https://doi.org/10.1016/j.gde.2015.12.003

Zhang, M., Jungblut, A., Kunert, F., Hauptmann, L., Hoffmann, T., Kolesnikova, O., Metzner, F., Moldt, M., Weis, F., DiMaio, F., Hopfner, K.-P., Eustermann, S., 2023. Hexasome-INO80 complex reveals structural basis of noncanonical nucleosome remodeling. Science 381, 313–319. https://doi.org/10.1126/science.adf6287

Zhu, F., Farnung, L., Kaasinen, E., Sahu, B., Yin, Y., Wei, B., Dodonova, S.O., Nitta, K.R., Morgunova, E., Taipale, M., Cramer, P., Taipale, J., 2018. The interaction landscape between transcription factors and the nucleosome. Nature 562, 76–81. https://doi.org/10.1038/s41586-018-0549-5

Table I

Table for H2A and H2B solvation free energy and interface area interacting with DNA. The data is obtained using PISA (Krissinel and Henrick, 2007) and the nucleosome-only control is 6FQ5 (Bilokapic et al., 2018).

	ΔG (kcal/mol)		interface area (Å^2)	
	ELF2-nuc	nuc	ELF2-nuc	nuc
H2A interaction with + strand	-1.7	-3.5	79.9	531.5
H2A interaction with - strand	-	-5.8	-	504.9
H2B interaction with + strand	-3.1	-5	161.2	440.7
H2B interaction with - strand	-0.2	-6.5	38.5	400.1

FIGURE LEGENDS

Figure 1. ELF2 displays high orientational and positional specificity on nucleosomal DNA.
A: preferred ELF2 binding position on the nucleosome (data from (Zhu et al., 2018)). Dark and light blue circles represent binding in plus and minus strands, respectively. Note that ELF2 has a strong oriented binding preference on the plus strand at 108 bp (near SHL +4).
B: DNA ligand design. Cartoon shows Widom 601 core sequence (147bp) with ELF2 double motif (CCGGAAGCGGAAGT) inserted in the most preferred binding position. Numbers indicate superhelical location.
C: Positions of the two GGAA core binding sequences of ELF-HT2 on the nucleosome. The DNA sequence from 6FQ5 was mutated to the designed sequence using coot. The image is acquired using ChimeraX. Blue: H3; Green: H4; Yellow: H2A; Red: H2B.

Figure 2: The structure of ELF2-bound nucleosome.
A: ELF2-nucleosome composite cryo-EM map.
B: ELF2-nucleosome model.
C: ELF2-nucleosome model rotated; top -90° Z; bottom -90° X from top.
D: Local ELF2-nucleosome interaction. ELF2 DBDs are docked into the CCGGAAGCGGAAGT binding motif. Right image is 90° rotation around the y axis from the left.

Figure 3: ELF2 unwraps nucleosome, resulting in hexasome formation.
A: ELF2-nucleosome model overlaid on a canonical nucleosome (6FQ5 DNA shown in gray). Dyad axis is labelled. The nucleosome is unwrapped at around superhelical location +4 where ELF2 binds. The engineered EcoRV cleavage site is indicated. The model was extended in Coot with ideal B-form DNA on the unwrapped end to represent the full 147 bp DNA ligand.
B: Restriction enzyme digestion assay. Asterisks indicate lanes with faster-migrating DNA bands (DNA cleaved by EcoRV). Samples were denatured before gel electrophoresis.
C: Side view of ELF2-nucleosome interaction with K229 and K239 highlighted with the potential phosphate backbone interaction indicated by dotted lines.
D: H2A:H2B dimer exposed by DNA unwrapping.

E: Contacts between H2A:H2B and DNA that are lost after unwrapping (indicated by orange spheres).

F: Structure of ELF2-bound hexasome. Cryo-EM map with canonical nucleosome (6FQ5) fitted is shown.

Figure 4: Potential role of ELF2-HT2 motif in facilitating transcription initiation.

A: Enrichment of ELF2-HT2 motif downstream of TSS. Metagene plot of the enrichment of the indicated TF motifs relative to the TSS positions in the human genome (hg38). Distance from TSS against motif count in a 10 bp sliding window is shown. DNA that would be made accessible by nucleosome unwrapping is highlighted by green shading.

B: Model of DNA unwrapping and transcriptional regulation by ELF2. ELF2 binding unwraps the nucleosome by about 40bp. ELF2 motifs are enriched near the TSS and oriented so that unwrapping after binding would make the TSS accessible. In addition, ELF2 promotes formation of hexasomes.

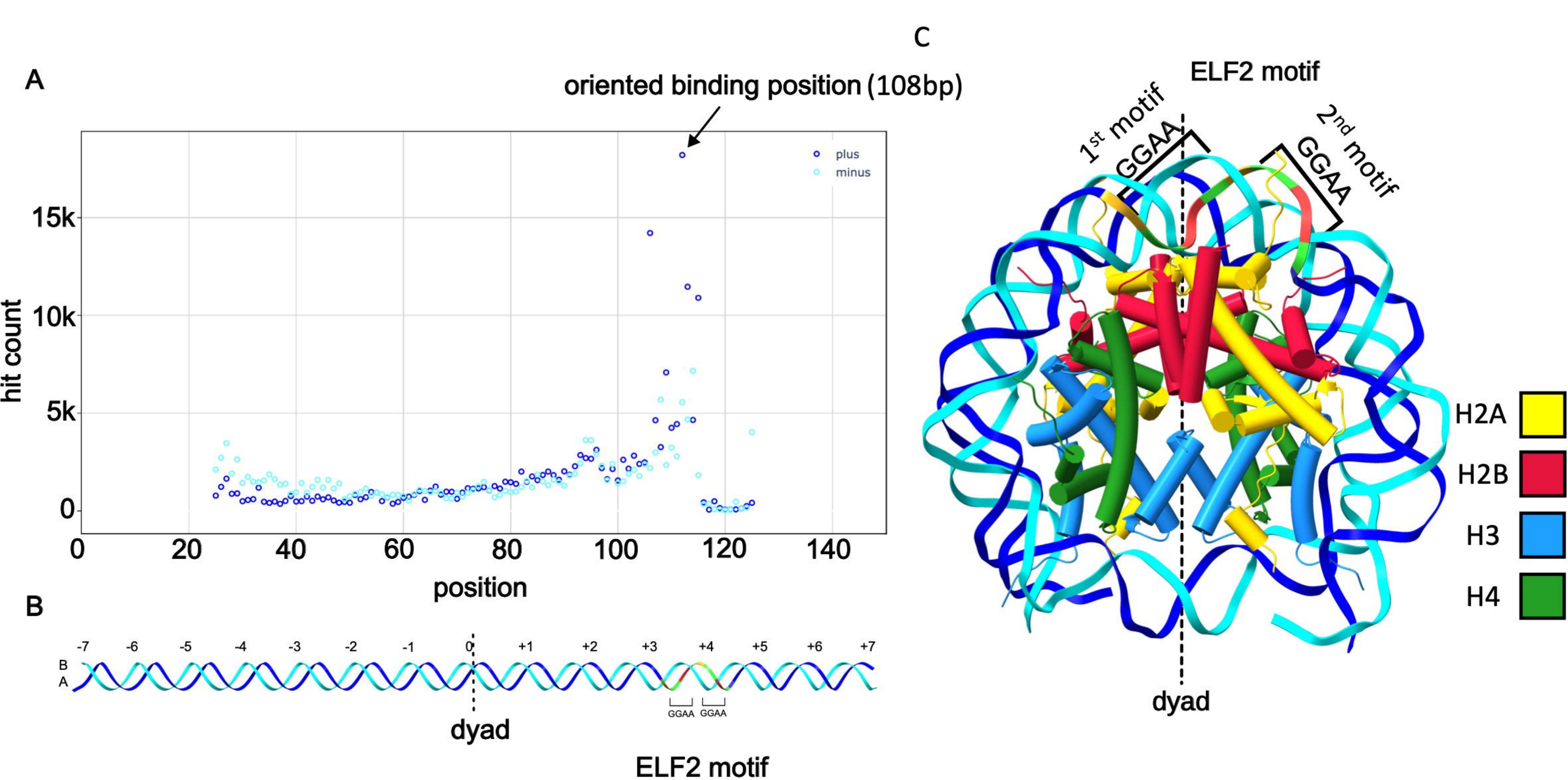
A
oriented binding position (108bp)
plus
minus
hit count
15k
10k
5k
0
0
20
40
60
80
100
120
140
position
B
-7
-6
-5
-4
-3
-2
-1
0
+1
+2
+3
+4
+5
+6
+7
B
A
GGAA
GGAA
dyad
ELF2 motif
C
ELF2 motif
1st motif
GGAA
2nd motif
GGAA
dyad
H2A
H2B
H3
H4

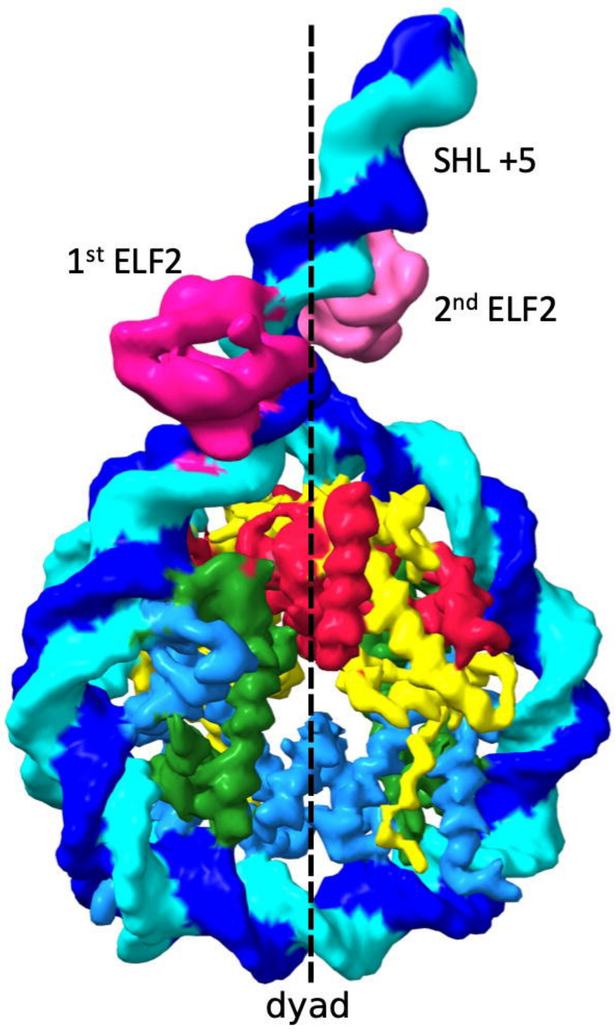
A
SHL +5
1st ELF2
2nd ELF2
dyad

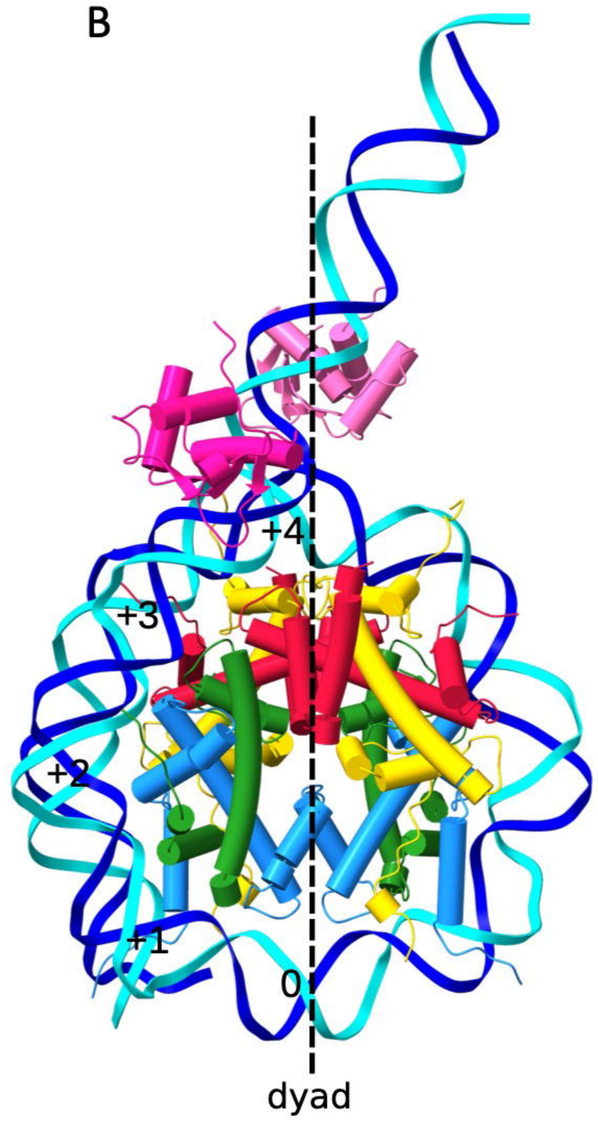
B
+4
+3
+2
+1
0
dyad

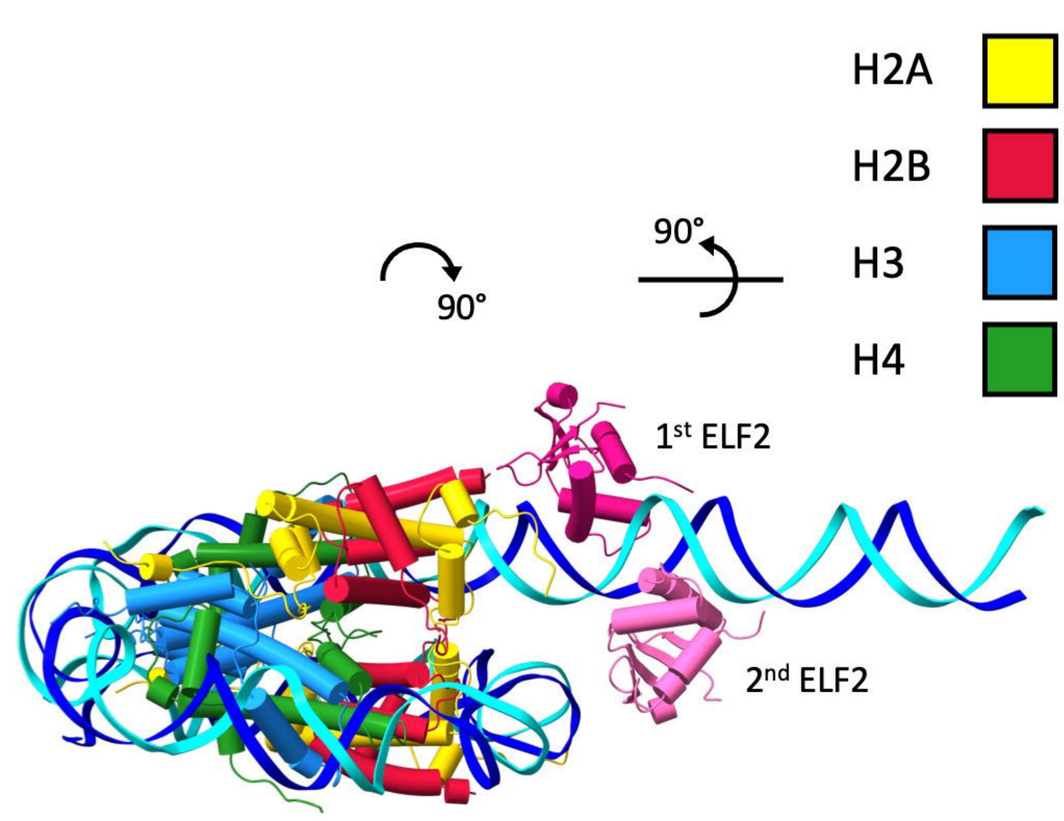
C
H2A
H2B
H3
H4
90°
90°
1st ELF2
2nd ELF2

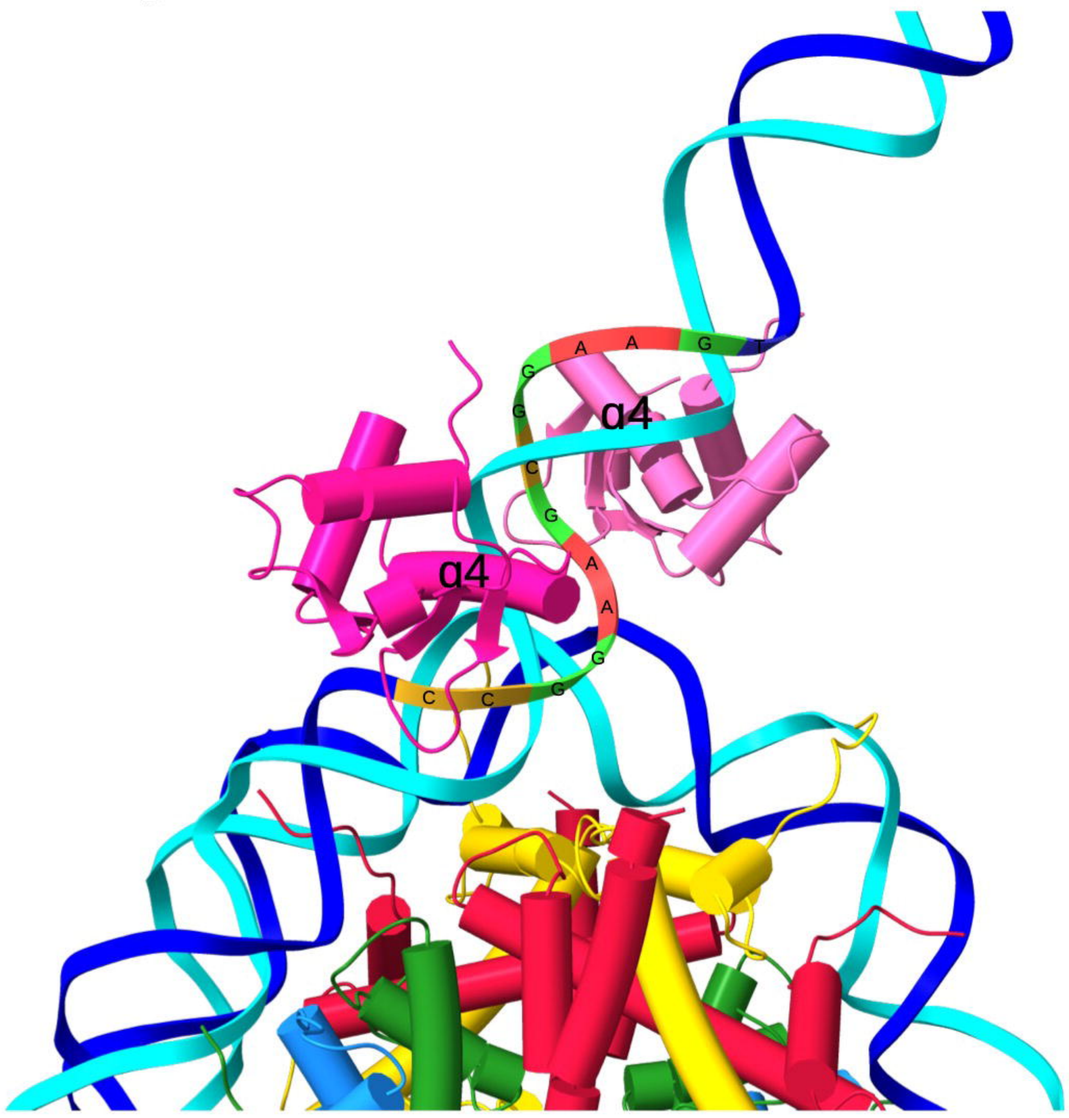
D
α4
α4

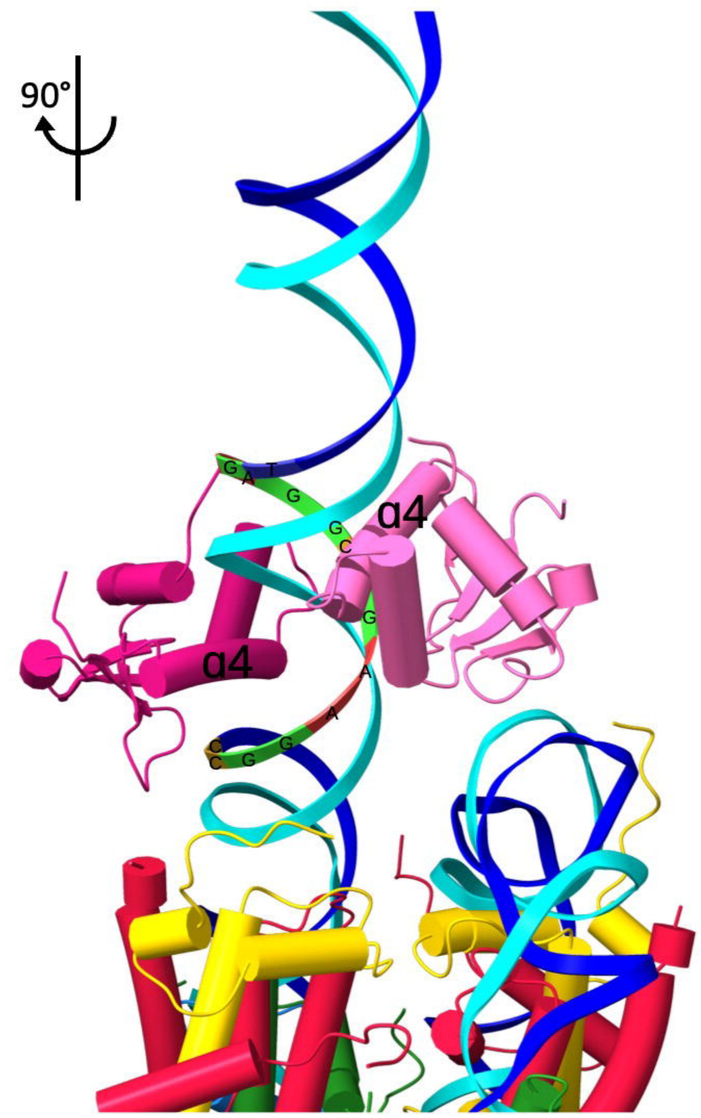
90°
α4
α4

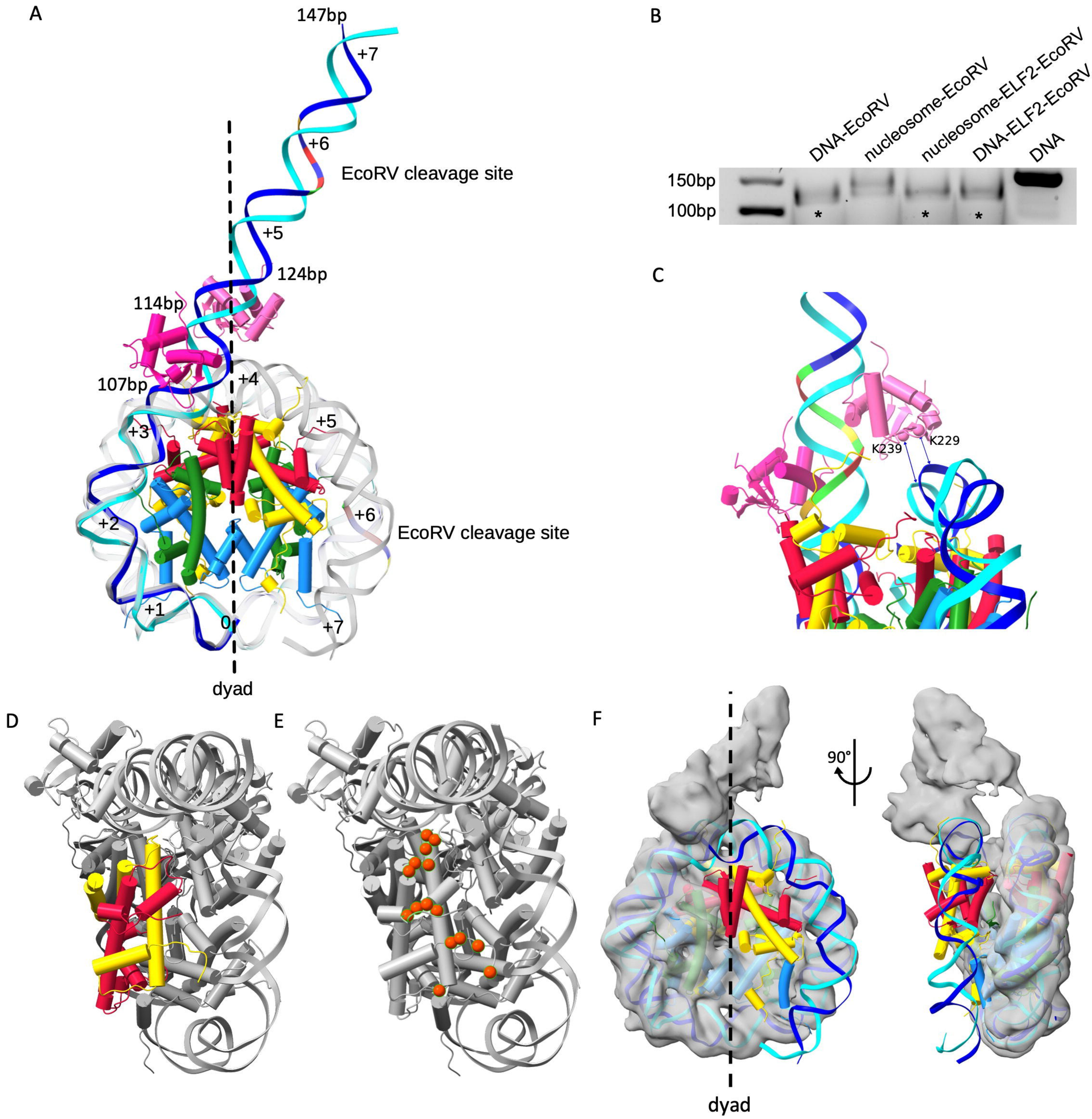
A
147bp
+7
+6
EcoRV cleavage site
+5
124bp
114bp
107bp
+4
+3
+5
+2
+6
EcoRV cleavage site
+1
0
+7
dyad
B
DNA-EcoRV
nucleosome-EcoRV
nucleosome-ELF2-EcoRV
DNA-ELF2-EcoRV
DNA
150bp
100bp
*
*
*
C
K239
K229
D
E
F
90°
dyad

A

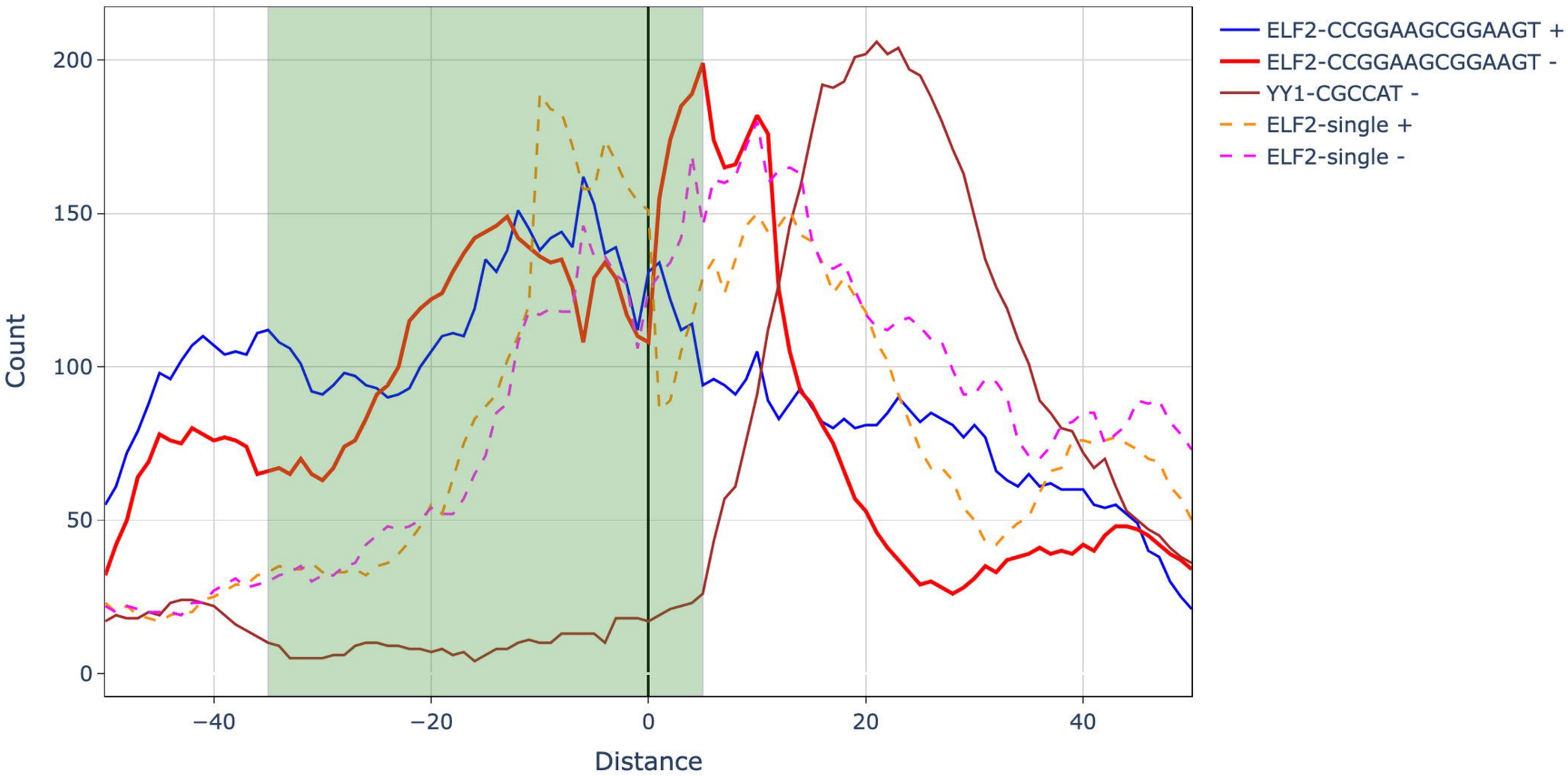
ELF2-CCGGAAGCGGAAGT +
ELF2-CCGGAAGCGGAAGT -
YY1-CGCCAT -
ELF2-single +
ELF2-single -
Count
200
150
100
50
0
−40
−20
0
20
40
Distance

B

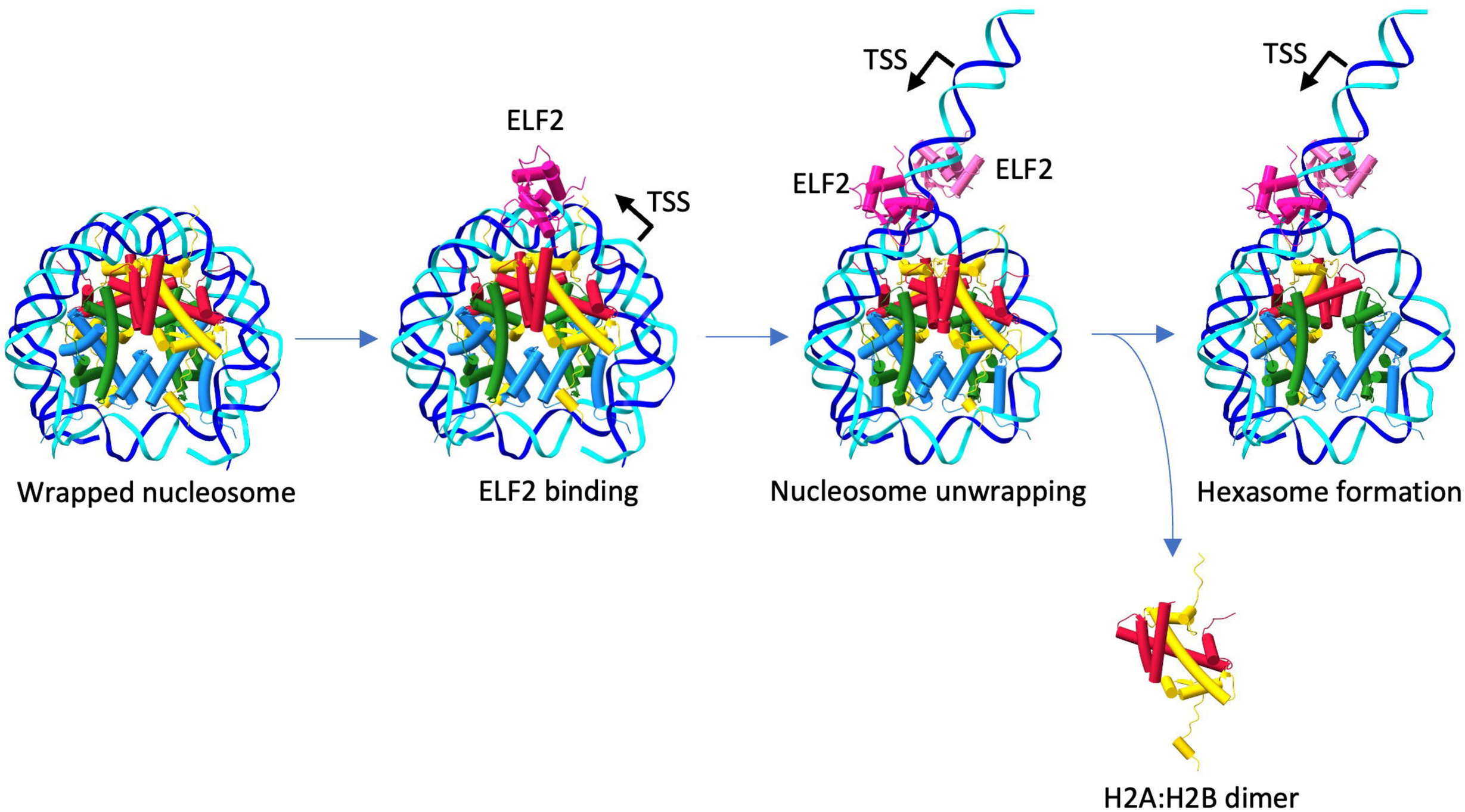
ELF2
TSS
TSS
ELF2
ELF2
TSS
Wrapped nucleosome
ELF2 binding
Nucleosome unwrapping
Hexasome formation
H2A:H2B dimer